International Journal of Science and Research (IJSR)
ISSN (Online): 2319-7064, Impact Factor (2013): 4.438
www.ijsr.net

Photoacoustic Image Simulation of Ensemble of Light Absorbing Cells using Linear Array Transducer

Subhajit Karmakar[1] and Ratan K Saha[2]

[1]University Science Instrumentation Centre, The University of Burdwan, Bardhaman 713104, West Bengal, India

[2]Surface Physics and Material Science Division, Saha Institute of Nuclear Physics,1/AF Bidhannagar, Kolkata 700064, India

Abstract: ***Recently, we developed a theoretical framework to study photoacoustics (PAs) from an ensemble of cells. PA field from a single cell approximated as a fluid sphere and suspended in a non-absorbing fluid medium has been calculated by employing a frequency domain approach and that for many cells has been computed by linearly adding the fields emitted by the individual cells. This model has been extended here to simulate PA images of various tissue mimicking phantoms composed of collections of cancer cells containing gold nano-particles and red blood cells using linear array transducer. The simulated images were found to correlate well with the numerical phantoms and that validated the approach illustrated here. This methodology might offer an alternative as well as a realistic way to simulate PA images of an ensemble of regular PA objects.***

Keywords: Photoacoustic image simulation, linear array transducer, delay and sum beamforming, vasculature structure, tumour phantom, red blood cells, cancer cells, endocytosed gold nano-particles

1. Introduction

Photoacoustic (PA) imaging technique is a new hybrid imaging modality [1-3]. It has developed as a potential biomedical imaging modality over the last 15 years. It has been successfully utilized to visualize anatomy and functional states of various small animal organs. Optically induced ultrasonic waves are detected in this technique. Contrast in a PA image is governed by the optical contrast retained in the imaging medium. The resolution of an image is dictated by that of the ultrasonic receiver. Further, this technique has the ability to image deep tissue regions, where optical modalities do not work. This is because scattering of light is two to three orders of magnitude higher than that of ultrasonic waves. PA imaging technique is currently functional at two settings namely, PA microscopy and PA tomography (PAT). In PAT, using a linear or circular array operating at the frequency band 4 to 8 MHz imaging depth up to 7 cm can be achieved and also breast vasculature in a human volunteer could be imaged *in vivo* [3].

In addition to experimental works, PA image simulation is also an active research field. A numerical method known as k-Wave simulation tool box has been extensively used in PA image simulation studies [4]. It solves coupled partial differential equations of PA wave propagation using a Fourier transformation method. It has been used to study the influence of various parameters (laser fluence, transducer geometry, transducer frequency response etc.) on PA imaging. The performance of reconstruction algorithms for PAT applications has also been evaluated [5].

In this paper, we propose a new methodology for image simulation of collection of light absorbing fluid spheres. The mathematical model for PA emission by an ensemble of light absorbing fluid spheres was successfully explored in predicting blood oxygen saturation [6]. The methodology has been implemented here to simulate PA images of collections of cancer cells with endocytosed gold nano-particles (AuNPs) [7-8] and red blood cells (RBCs) using linear array transducer. It seems that the method has the potential to emerge as a realistic image simulation tool.

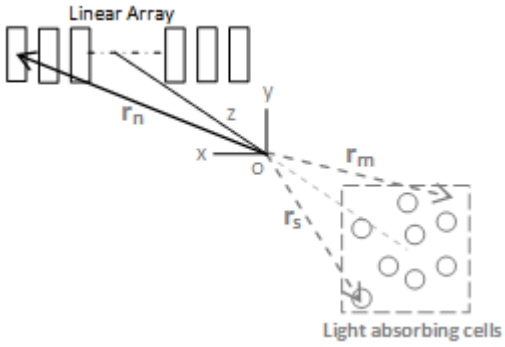

Figure 1: Schematic of PA imaging geometry.

2. Analytical Model

Modeling of PA field from a single spherical source: The time dependent wave equation for PA field can be derived from the linearized equations of fluid dynamics and by imposing the condition of thermal confinement. The solution to the wave equation for uniformly illuminated fluid sphere acting as a PA source is given by [9-10],

$$p(\mathbf{r}_n,\omega) = BI_0 p_s(\omega)\frac{e^{ik_f|\mathbf{r}_n-\mathbf{r}_s|}}{|\mathbf{r}_n-\mathbf{r}_s|}, \quad (1)$$

where $|\mathbf{r_n}-\mathbf{r_S}|$ is the distance between the observation point $\mathbf{r_n}$ and the center of PA source positioned at $\mathbf{r_S}$ as shown in Fig. 1, $B=\frac{i\mu\beta v_s a^2}{C_P}$ and

$$p_s(\omega) = \frac{j_1(\hat{q})e^{-ik_f a}}{[(1-\hat{\rho})\frac{\sin(\hat{q})}{\hat{q}}-\cos(\hat{q})+i\hat{\rho}\hat{v}\sin(\hat{q})]}, \quad (2)$$

where $\hat{q} = k_s a$ and j_1 represents the spherical Bessel function of the first kind of order unity. The dimensionless quantities, $\hat{\rho} = \rho_s / \rho_f$ and $\hat{v} = v_s / v_f$ indicate the density and the acoustic wave velocity for the absorber with respect to those for the suspending medium, respectively; k_s and k_f are the wave numbers for the acoustic wave inside and outside the source, respectively. The time dependent PA field for a delta function heating pulse can be derived by taking the inverse Fourier transform of Eq. 2 yielding [9-10],

$$p(\mathbf{r}_n, t) = \frac{BF}{2\pi}\int_{-\infty}^{\infty} d\omega\, p_s(\omega)\frac{e^{ik_f|\mathbf{r}_n - \mathbf{r}_s|}}{|\mathbf{r}_n - \mathbf{r}_s|}e^{-i\omega t}, \quad (3)$$

where F is the incident optical fluence. Eq. 3 represents an analytic signal. The contributions from all possible frequencies are added in Eq. 3

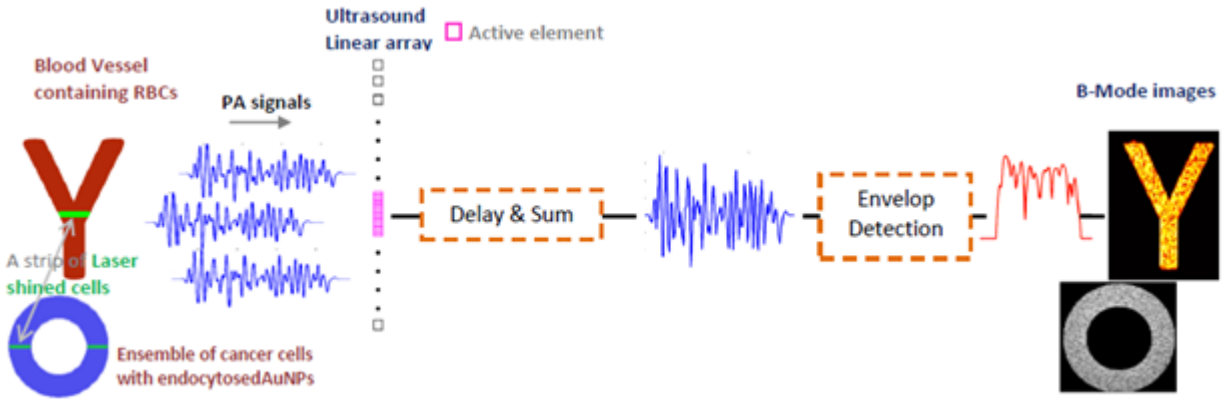

Figure 2: PA imaging using linear array and delay and sum beamforming

PA signal detected by a single element of the linear array transducer: The measured signal $p_s^n(t)$ by the n^{th} element of the linear array is proportional to PA pressure spatially averaged over the aperture area A of the element and it can be written as,

$$p_s^n(t) = \frac{BF}{2\pi A}\iint d^2\mathbf{r}_n \int_{-\infty}^{\infty} d\omega\, p_s(\omega)\frac{e^{ik_f|\mathbf{r}_n - \mathbf{r}_s|}}{|\mathbf{r}_n - \mathbf{r}_s|}e^{-i\omega t}$$

$$= \frac{BF}{A}\int_{-\infty}^{\infty} d\omega e^{-i\omega t}\, p_s(\omega) H_D(\mathbf{r}_n, \omega), \quad (4)$$

where $H_D(\mathbf{r}_n, \omega) = \iint \frac{e^{i\omega/v_f|\mathbf{r}_n - \mathbf{r}_s|}}{2\pi|\mathbf{r}_n - \mathbf{r}_s|} d^2\mathbf{r}_n$ represents the directivity function of the transducer. Using the property of the Fourier transformation the above equation can be equivalently expressed as

$$p_s^n(t) = \frac{2\pi}{A}[p_s(t) *_t h(\mathbf{r}_s, t - |\mathbf{r}_n - \mathbf{r}_s|/v_f)], \quad (5)$$

where $p_s(t) = \frac{BF}{2\pi}\int_{-\infty}^{\infty} d\omega\, p_s(\omega)e^{-i\omega t}$, $*_t$ denotes temporal convolution and $h(\mathbf{r}_s, t) = \iint \frac{\delta(t - |\mathbf{r}_n - \mathbf{r}_s|/v_f)}{2\pi|\mathbf{r}_n - \mathbf{r}_s|} d^2\mathbf{r}_n$ represents the spatial impulse response function (SIRF) of the acoustic receiver. For an ensemble of monodisperse absorbers having similar biophysical and biochemical conditions, the resultant signal can be written as a linear superposition of tiny signals emitted by the individual sources,

$$P_n(t) = \sum_s p_s^n(t). \quad (6)$$

The corresponding geometry is displayed in Fig. 1. Eq. 6 represents a complex signal, however, PA pressure signals are real and detected by an ultrasound transducer with finite receiving bandwidth. The frequency response of a transducer can suitably be modeled using the Gaussian functions for which time domain impulse response be expressedas,

$$g_R(\omega_0, \xi, t) = \frac{\xi}{\sqrt{2\pi}} e^{-\frac{\xi^2 t^2}{2}} \cos(\omega_0 t) \quad (7)$$

$$g_I(\omega_0, \xi, t) = \frac{\xi}{\sqrt{2\pi}} e^{-\frac{\xi^2 t^2}{2}} \sin(\omega_0 t) \quad (8)$$

where ω_0 is the center frequency and ξ is the -6 dB bandwidth. A bandlimited (BL) radio frequency (RF) signal $p_n^{BL}(t)$ for the nth element can be calculated by convoluting the real part of $P_n(t)$ with g_R as,

$$p_n^{BL}(t) = Re\{P_n(t)\} *_t g_R(\omega_0, \xi, t). \quad (9)$$

Delay and sum beamforming: A linear array consists of periodically arranged N number of small active elements. Out of which a group of N_A elements are used for dynamically focus a space point and construct a beamformed RF line for imaging. It is evident from the array geometry (see Fig. 1) that PA signal $p_n^{BL}(t)$ originating from a source location at $\mathbf{r}_m$ arrives the n^{th} element at time $t_m = \frac{|\mathbf{r}_n - \mathbf{r}_m|}{\mathbf{v_f}}$. But, the signal will be delayed by an amount of $\tau_n = \frac{|\mathbf{r}_{n+1} - \mathbf{r}_m| - |\mathbf{r}_n - \mathbf{r}_m|}{\mathbf{v_f}}$ to reach the

$n+1^{th}$ element of the array due to the path difference between source to observation points at two different elements. Therefore, to focus a space point $\mathbf{r}_m$, relative delays between the group of active array elements need to be compensated before adding their responses with different weights W_n. The resultant PA pressure under delay and sum beamforming can be written as,

$$p(t_m) = \sum_{n=0}^{N_A-1} W_n \, p_n^{\mathrm{BL}}(t_m - \tau_n) \tag{10}$$

and consequently the beamformed RF line for many such spatial source locations can be found as,

$$p^{\mathrm{BF}}(t) = \sum_{n=0}^{N_A-1} W_n \, p_n^{\mathrm{BL}}(t - \tau_n). \tag{11}$$

The envelope of the beamformed line can be obtained using the BL Hilbert transformer of Eq. 7 and 8 as

$$E(t) = \sqrt{\left(p^{\mathrm{BF}}(t) *_t g_R\right)^2 + \left(p^{\mathrm{BF}}(t) *_t g_I\right)^2}. \tag{12}$$

Eq. 12 has been calculated in this study to simulate envelopes of bandlimited RF lines for light absorbing cells and detected by linear array transducer.

3. Materials and Methods

Phantom generation and cell parameters

A numerical O-shaped phantom was constructed using NP filled cells randomly positioned inside a volume of 7 x 0.5 x 5 mm^3. Each cell was treated as a fluid sphere with radius $a = 5$ µm mimicking human epithelial carcinoma cells (A431 keratinocyte). These cells enclosed Au nanospheres with radius 25 nm. The volume fraction occupied by cells was 20×10^4 cells/ml. The plasmon resonance peak for such NPs appears around 532 nm, where light absorption is maximum. The absorption efficiency was computed as 3.297 at 532 nm and accordingly, μ was found to be 5600464.9 m^{-1} for a concentration of NPs of about 45.3×10^4 NPs/cell [11]. The choices of the cell line and physical parameters were made based on the experimental data [12]. The random locations of cells within the O-shaped region were generated using a Monte Carlo technique. The density and the speed of sound for cell were taken as $\rho_s = 1090$ $\mathrm{kg/m}^3$ and $v_s = 1535$ m/s, respectively. The thermal expansion coefficient and isobaric specific heat of the cellular medium and fluence of the optical beam were treated as constant since these parameters essentially control amplitude of the signal and do not affect its frequency content. The density and the speed of sound for the surrounding medium were fixed to $\rho_f = 1005$ $\mathrm{kg/m}^3$ and $v_f = 1540$ m/s, respectively. Another numerical phantom was constructed by placing a Y-shaped region inside a volume of 7 x 0.5 x 5 mm^3. The Y-shaped region was filled with randomly positioned RBCs of radius 2.75 µm. It could be thought to be a branch of a vascular network. The concentration of RBCs or the hemtocrit level was chosen only 1 % which is far below the physiological limit. This concentration was fixed to appreciate speckle structure in PA image. The μ for a RBC at 532 nm was considered to be 53958.8 m^{-1}.

Array specifications

A 128 element linear array transducer of center frequency 40 MHz was used to detect PA signals. The size of each array element was taken as 38.5- x 385- µm and the spacing between two adjacent elements was fixed at 19.25 µm. A beamformed line was constructed using a sub-aperture consisting of 16 elements.

Imaging algorithm

A 532 nm laser beam propagated along the y-direction and uniformly illuminated a volume of 7 x 0.5 x 0.062 mm^3. The irradiated region is highlighted in figure (see Fig. 2). PA waves, emitted by cells in that irradiated volume and propagated along the z-direction, were received by the sub-aperture of the linear array transducer. PA signal was computed by convolving the collective signal emitted by those cells with SIRF of the array elements. A well-known software Field II was employed to calculate SIRF for the transducer used. BL transducer response was obtained according to Eq. 9. The Gaussian window of the filtering functions was truncated up to $\pm 4/\xi$ length. Each BL RF line was further decimated by a factor of 20 while performing delay and sum operations over the individual PA signals received by the elements in the sub-aperture. Initially, 113 such scan lines along the x-direction were computed for the entire phantom volume. The envelope of each BF scan line was determined using the Hilbert transform pairs as given Eq. 12. Log compression and interpolation along the x-direction had been used to obtain a 40 dB dynamic range B-Mode PA image of the numerical phantoms. 256 gray levels were used to encode the dynamic range.

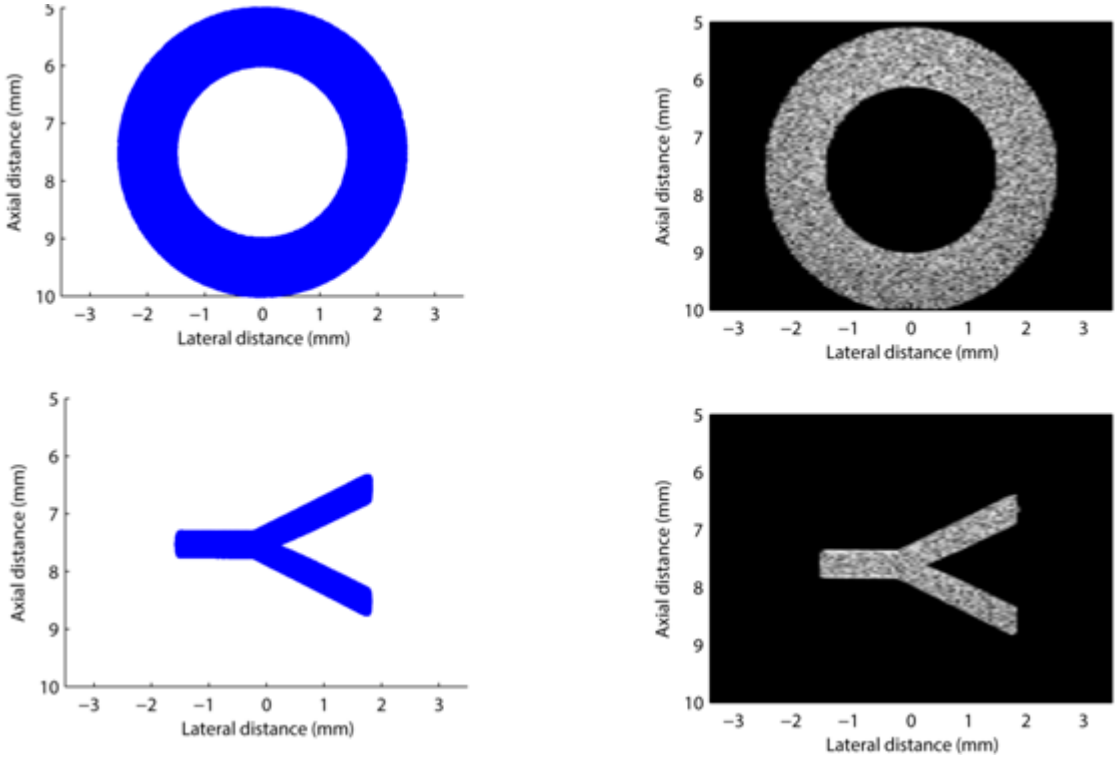

Figure 3: Numerical phantoms (left column) and their corresponding simulated PA images (right column).

4. Results and Discussion

B-mode images of the phantoms depicted in Fig. 2 are shown in Fig. 3. The simulated images were found to correlate well with the O- and Y-shaped phantoms that validated the approach illustrated here. The presence of speckles was apparent in the simulated images (see Fig. 3 right column). This is unlike to appear in the PA images generated experimentally [1-3]. The speckle free images have been obtained under experimental condition because concentrations of light absorbing cells containing chromophores inside the source region have been higher compared to that of outside. The concentration difference and coherent addition produce very strong signal at the boundary which finally suppresses small amplitude details in the finite dynamic range gray scale images. In the present study, the concentrations of cells were chosen suitably low to minimize the boundary effect so that the contribution of incoherent addition of PA signals from tiny cells which generated speckle became noticeable in the gray image..

As discussed earlier, the k-Wave method has been extensively used in this field to simulate PA images of regular and irregular absorbing structures. This technique numerically solves coupled partial differential equations for wave propagation to obtain time evolution of PA field. It is a well-known fact that the k-Wave method is a time consuming and memory intensive process. The methodology discussed in this work is a computationally less expensive procedure but it is applicable for samples composed of regular PA sources.

5. Conclusions

A PA image simulation methodology is described in this paper. It approximates a tissue as a collection of cells. These cells generate acoustic waves upon optical illumination if they enclose light absorbing molecules. PA signals emitted by individual cells were linearly superposed to obtain a PA RF line. The detailed derivation of the delay and sum beamforming technique associated with linear array transducer is presented. This technique was implemented in this work to generate PA images of numerical phantoms consisting of cancer cells encapsulating AuNPs and RBCs. The simulated images demonstrate good correlation with the phantoms validating the methodology presented here. This approach might offer an alternative as well as a realistic way to simulate PA images of an ensemble of regular PA objects.

Acknowledgements

R K Saha expresses his thank to CSIR, New Delhi for funding.

References

[1] **Beard P.**, Biomedical photoacoustic imaging, *Interface Focus*, **1**, 602-631, 2011.
[2] **Zhang H. F.**, **Maslov K.**, **StoicaG.**, and **Wang L. V.**, Functional photoacoustic microscopy for high-resolution and noninvasive*in vivo* imaging, *Nature Biotechnology*, **24**(7), 848-851, 2006.
[3] **Wang L. V.** and **Hu S.,** Photoacoustic Tomography: In Vivo Imaging from Organelles to Organs, *Science*, **335**, 1458-1462, 2012.
[4] **Treeby B. E.**, and **Cox B. T.**, k-Wave: MATLAB toolbox for the simulation and reconstruction of photoacoustic wave fields, *Journal of Biomedcial Optics*, **15**(2), 021314, 2010.
[5] **Shaw C. B.**, **Prakash J.**, **Pramanik M.**, and **Yalavarthy P. K.**, Least-sqares QR-based decomposition an efficient way of computing and optimal regularization parameter in photoacoustic

tomography", *Journal of Biomedcial Optics*, **18**(8), 080501, 2013.

[6] **Saha R. K.** and **Kolios M. C.**, Effects of erythrocyte oxygenation on optoacoustic signals, *J. Biomed. Opt.*,**16**(11), 115003, 2011.

[7] **Mallidi S.**, **Joshi P. P.**, **Sokolov K.**, and **Emelianov S. Y.**, On sensitivity of molecular specific photoacoustic imaging using plasmonic gold nanoparticles, *Proc. of IEEE EMBS*, 6338-6340, 2009.

[8] **Eghtedari M.**, **Motamedi M.**, **Popov V.L.**, **Kotov N.A.**, and **Oraevsky A. A.**, Optoacoustic imaging of gold nanoparticles targeted to breast cancer cells, *Proc. of SPIE***, 5320,** 21-28, 2004.

[9] **Diebold G. J.**, **Sun T.**, and **Khan M. I.**, Photoacoustic monopole radiation in one, two and three dimensions, *Phys. Rev. Lett.*, **67**(24), 3384-3387, 1991.

[10] **Saha R. K.** and **Kolios M. C.**, A simulation study on photoacoustic signals from red blood cells, *J. Acoust. Soc. Am.*, **129**, 2935-2943, 2011.

[11] **Saha R.K.**, Roy M., and Datta A., Simulation study on the photoacoustics of cells with endocytosed gold nanoparticles, *Current Science*, **106**(11), 1554-1559, 2014.

[12] **Nam S. Y.**, **Ricles L. M.**, **Suggs L. J.**, and **Emelianov S. Y.**, Nonlinear photoacoustic signal increase from endocytosis of gold nanoparticles, *Opt. Lett.*, **37**(22), 4708-4710, 2012.